Magnetic ordering and dynamics in the XY pyrochlore antiferromagnet: a muon-spin relaxation study of $Er_2Ti_2O_7$ and $Er_2Sn_2O_7$

2005 J. Phys.: Condens. Matter 17 979

(http://iopscience.iop.org/0953-8984/17/6/015)

INSTITUTE OF PHYSICS PUBLISHING JOURNAL OF PHYSICS: CONDENSED MATTER

J. Phys.: Condens. Matter **17** (2005) 979–988 doi:10.1088/0953-8984/17/6/015

Magnetic ordering and dynamics in the XY pyrochlore antiferromagnet: a muon-spin relaxation study of $Er_2Ti_2O_7$ and $Er_2Sn_2O_7$

J Lago[1,5], T Lancaster[2], S J Blundell[2], S T Bramwell[1], F L Pratt[3], M Shirai[1] and C Baines[4]

[1] Department of Chemistry, University College London, 20 Gordon Street, London WC1H OAJ, UK
[2] Clarendon Laboratory, Department of Physics, Oxford University, Parks Road, Oxford OX1 3PU, UK
[3] ISIS, Rutherford Appleton Laboratory, Chilton, Didcot OX11 0QX, UK
[4] Paul Scherrer Institut, Laboratory for Muon Spin Spectroscopy, CH-5232 Villigen PSI, Switzerland

E-mail: j.lago@ucl.ac.uk

Received 9 September 2004, in final form 8 November 2004
Published 28 January 2005
Online at stacks.iop.org/JPhysCM/17/979

Abstract

Spin dynamics in $Er_2Ti_2O_7$ and $Er_2Sn_2O_7$ have been probed by means of muon-spin relaxation (μ^+SR) in the temperature range $0.02 \leqslant T \leqslant 300$ K. Both compounds are thought to constitute experimental realizations of the highly frustrated XY antiferromagnet on the pyrochlore lattice, for which theory predicts fluctuation-induced magnetic order. Our results for $Er_2Ti_2O_7$ are consistent with a transition into an ordered state at $T_N \sim 1.1$ K, in agreement with previous neutron measurements. Below this temperature, the muon relaxation rate $\lambda(T)$ remains large ($\sim$2 MHz) and temperature independent, in contrast to the behaviour in conventional magnets. The thermal evolution of $\lambda(T)$ for $Er_2Sn_2O_7$ is somewhat similar to that of the Ti material. However, the depolarization curves remain exponential over the entire temperature range, suggesting a dense distribution of rapidly fluctuating magnetic moments, and, thus, are compatible with the absence of long-range order at least for $T > 0.02$ K.

(Some figures in this article are in colour only in the electronic version)

1. Introduction

Geometrical frustration arises in magnetic systems when symmetry incompatibility exists between the local antiferromagnetic coupling and the topology of a triangular-based lattice.

[5] Author to whom any correspondence should be addressed.

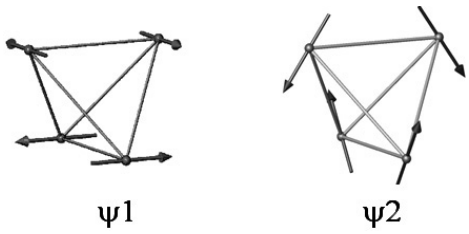

Figure 1. Tetrahedral basis of the pyrochlore lattice indicating two possible ground states of the $\langle 111 \rangle$ easy-plane antiferromagnet, equation (1), as described in [5]. State ψ_2 (with propagation vector $Q = 0$) is selected by thermal fluctuations and observed experimentally in $Er_2Ti_2O_7$.

This prevents all pairwise spin interactions from being simultaneously satisfied and can lead to a large ground state degeneracy so that, in principle, the system remains disordered as $T \to 0$. In real systems, however, perturbative terms in the Hamiltonian are able to select a smaller subset of ground states whose nature depends on the specific material in question. The result is the rich variety of low temperature behaviour encountered experimentally.

In the pyrochlore titanates $RE_2Ti_2O_7$ (RE = rare-earth) the magnetic rare earth ions occupy a pyrochlore lattice of corner-linked tetrahedra. Magnetic moments are coupled together by exchange and dipolar interactions and experience strong single ion anisotropy arising from the combined effect of the local crystal field and spin orbit coupling. The role of the anisotropy term is particularly significant: whereas the pure Heisenberg antiferromagnet has a spin-liquid low temperature state [1], strong easy-axis anisotropy directed along the local trigonal axes (members of the $\langle 111 \rangle$ set that connect the centre of the elementary tetrahedron to its vertices) leads to the disordered, macroscopically degenerate 'spin ice' state found for RE = Ho^{3+} and Dy^{3+}, with effective ferromagnetic coupling [2, 3].

For the pyrochlore antiferromagnet with local $\langle 111 \rangle$ easy-plane anisotropy, with spins lying on easy planes perpendicular to the $\langle 111 \rangle$ local axes (see figure 1), an appropriate classical Hamiltonian is [4, 5]

$$H = -J \sum_{\langle i,j \rangle} \vec{S}_i \cdot \vec{S}_j - D \sum_i (\vec{S}_i \cdot \vec{\delta}_i)^2, \tag{1}$$

where $\delta_i = \langle 111 \rangle$, $D < 0$ defines the anisotropy and $J < 0$ is the Heisenberg exchange. This Hamiltonian has a macroscopically degenerate set of ground states at $T = 0$. However, numerical simulations with large D/J indicate that a first order transition into a long-range ordered state with ordering wavevector $Q = 0$ occurs at $T_N/J \sim 0.1$, indicating a thermal ground state selection [4]. A classical spin wave analysis for $D = \infty$ shows that the selected ordered phase (ψ_2 in figure 1) is associated with a macroscopic number of soft modes over an extensive region of the Brillouin zone [6], consistent with an 'order by disorder' ordering mechanism [7]. Interestingly, the selected state differs from those favoured by dipolar interactions (ψ_1 in figure 1) and exchange terms beyond nearest neighbour (see [5]).

$Er_2Ti_2O_7$ constitutes a good approximation to the $\langle 111 \rangle$ XY antiferromagnet. It orders at $T_N = 1.173(2)$ K [5] into the expected ψ_2 state shown in figure 1. The ordered moment at 50 mK is $3.01(5)\mu_B/Er^{3+}$, in good agreement with a crystalline electric field (CEF) analysis that predicts a Kramers doublet ground state with the Er^{3+} moments lying almost perfectly perpendicular to the local $\langle 111 \rangle$ axes [8]. However:

(i) The transition is continuous (critical exponent $\beta = 0.33(2)$, characteristic of a 3D XY system), not first order as theoretically predicted.

(ii) Theory predicts a constant density of low-lying excitations, incompatible with the observed $\propto T^3$-dependence of the heat capacity below 1 K [5].
(iii) Quasielastic neutron scattering results suggest the existence of a gap in the excitation spectrum [5], incompatible with the classical model.
(iv) Specific heat [9] and susceptibility [10] results on isostructural Er_2GaSbO_7 and $Er_2Sn_2O_7$, which might be expected to be described by a similar Hamiltonian to that in equation (1), suggest that these materials do not order above 0.1 K.

Thus, despite its significant achievement in predicting the magnetically ordered state, the current classical model fails to provide a satisfactory interpretation for the excitation spectrum of $Er_2Ti_2O_7$ and to account for the behaviour of Sn and Sb–Ga compounds. The origin of this disagreement is most likely the failure of the classical model to account for the quantum mechanical excitations of the system: the single ion ground state is a doublet of XY-like nature, but in no sense classical.

Here we present results of a μ^+SR study of the compounds $Er_2Ti_2O_7$ and $Er_2Sn_2O_7$ that agree with previous results regarding ordering and provide further information on the dynamic nature of the low temperature regime for both materials. The paper is structured as follows: section 2 describes the experimental details, sections 3–5 contain the results and discussion, and section 6 is a conclusion.

2. Experimental details

Zero-field (ZF) measurements were performed on polycrystalline samples (synthesized from stoichiometric mixtures of the corresponding binary oxides at 1400 °C) using the GPS spectrometer and the LTF spectrometer at the Paul Scherrer Institute (PSI, Villigen, Switzerland) muon facility. The temperature range used was $0.02 < T < 300$ K. Additional longitudinal field (LF) measurements were performed on the MuSR spectrometer at the ISIS (RAL, UK) facility. In a μ^+SR experiment (for a review of the technique see, for example, [11]), almost 100% polarized positive muons are implanted in the samples where, after a short thermalization ($<10^{-10}$ s), they start precessing about the local magnetic fields. In their decay (with decay constant $\tau = 2.2 \times 10^{-6}$ s) a positron is emitted preferentially in the direction of the muon-spin direction at the instant of decay. The time histograms of positron counts, $N_F(t)$ and $N_B(t)$, collected in detectors placed in the forward (F) and backward (B) positions relative to the initial muon polarization thus measure the time evolution of the muon polarization. The muon-spin relaxation function (or *asymmetry*) $A(t)$ is given by

$$A(t) = \frac{N_B(t) - \alpha N_F(t)}{N_B(t) + \alpha N_F(t)} = a_0 P_z(t) + a_{bg}, \tag{2}$$

where a_0 is the initial asymmetry (which, for both ETO and ESO, was found to essentially remain unchanged from the high temperature values down to the lowest temperature) and $P_z(t)$ is the muon polarization in the specimen and provides information on the nature of the internal magnetic fields. The instrumental parameter α accounts for the relative F/B detector efficiencies and a_{bg} is the contribution from muons stopped outside the specimen. We now discuss the data in detail in sections 3–5.

3. High temperature behaviour: $T \gg 1$ K

ZF spectra for times $0 \leqslant t \leqslant 5$ μs are shown in figure 2, where the fit to a phenomenological 'power exponential' function $P_z(t) = \exp(-(\lambda t)^\beta)$ (solid curves) provides a simple way to

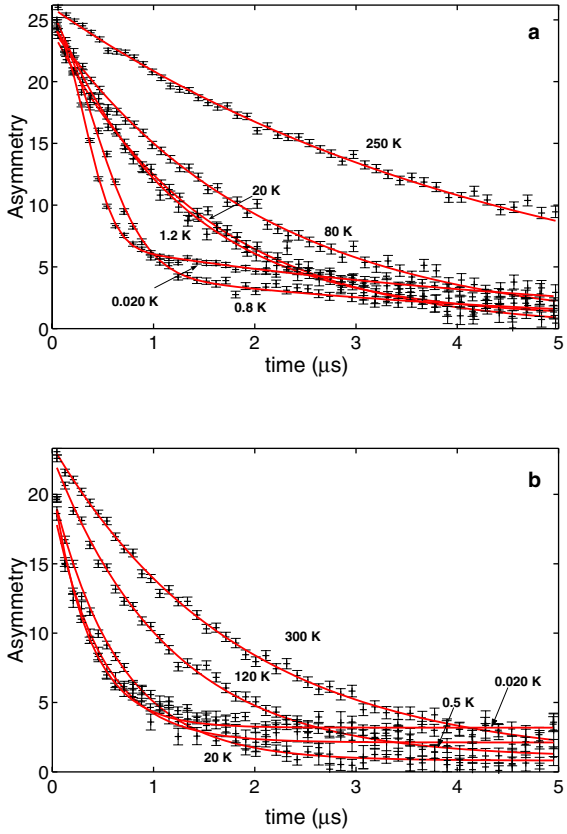

Figure 2. Raw μ^+SR data (PSI) for (a) $Er_2Ti_2O_7$ and (b) $Er_2Sn_2O_7$ at various temperatures. Solid curves are the fits to a stretched exponential relaxation function. Note that the apparent crossing of the curves that occur at low temperature for ESO results not from a change in their shape, but from the higher background level arising from the LTF dilution fridge.

parameterize the dynamic behaviour of these materials over the entire temperature range. The obtained temperature dependence of the relaxation rate λ is shown in figure 3 for both $Er_2Ti_2O_7$ (ETO) and $Er_2Sn_2O_7$ (ESO). At high temperatures the relaxation is described by a simple exponential ($\beta \simeq 1$) for both materials, as expected for a dense distribution of fast fluctuating electronic moments with a single fluctuation time (thus indicating that the Er^{3+} spin system dominates the observed depolarization of the muons). The thermal evolution of the estimated relaxation rate $\lambda(T)$ above the transition is reminiscent of that of the frustrated garnet $Yb_3Ga_5O_{12}$, [12] and suggests activated behaviour at high temperatures for both materials. We have fitted $\lambda(T)$ for $T > 5$ K to the expression $\lambda^{-1} = \lambda_0^{-1} + \eta \exp(-E_a/k_B T)$, where λ_0^{-1} is the value of saturation for $T < 30$ K and η reflects the strength of the spin–lattice interaction [12]. E_a is the energy, above that of the ground state, of the crystal field level that mediates the spin relaxation process. The fits (see figure 3) yield the values $\lambda_0^{-1} = 1.5(2)$ MHz^{-1}, $\eta = 4(1)$ MHz^{-1} and $E_a/k_B = 168(6)$ K for ETO and $\lambda_0^{-1} = 0.6(1)$ MHz^{-1}, $\eta = 2.0(8)$ MHz^{-1} and $E_a/k_B = 135(4)$ K for ESO, with the activation energy derived for ETO being much larger than the size of the gap to the two lowest excited CEF states derived from neutron scattering measurements, namely, 73 and 85 K [5] (no CEF data are available for ESO). The high temperature relaxation, therefore, cannot be explained by a single Orbach process [13, 14]

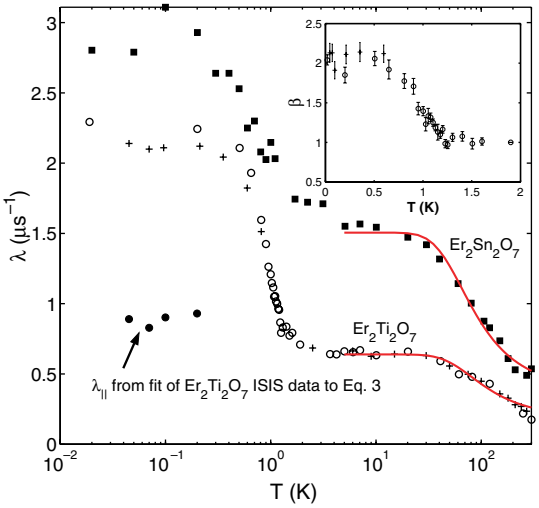

Figure 3. Relaxation rates λ derived from the fits of the raw spectra to a phenomenological stretched exponential function. Solid curves are the fit of the high temperature data to an exponential activation function (see the text). For ETO, PSI and ISIS data are represented by ○ and + respectively. $\lambda_{\|}$ is the longitudinal relaxation rate derived from fits of ISIS data to equation (3). Inset: thermal evolution of the power β for ETO showing the evolution from exponential to Gaussian curve shape across T_N. For ESO, $\beta = 1$ for the entire temperature range. The symbols have the same meaning as in the main figure.

involving the first CEF excited state as in the case of $Yb_3Ga_5O_{12}$ [12]. However, following [12], it still seems reasonable to discuss the present results in terms of a phonon-mediated mechanism and thus we argue that the relaxation above 30 K might imply not one but a combination of resonant processes[6] involving the states at $T \sim 80$ K as well as higher energy ones (note that an attempt to fit the data to a power law $\propto T^n$ yields a value of $n \sim 1$, inconsistent with a Raman process for a Kramers ion (for which $1/T_1 \propto T^n$ with $n = 9$ [15])). In the range $2 < T < 20$ K the relaxation rate is largely independent of temperature, suggesting a relaxation due to spin–spin exchange fluctuations once the Er^{3+} moments are confined to the ground state doublet.

4. Low temperature behaviour: $Er_2Ti_2O_7$

4.1. Muon site and the ordered phase

The sharp increase in $\lambda(T)$ observed at $T \sim 1$ K for ETO is consistent with the onset of the long-range AFM state as detected by neutron measurements, and reflects the slowing down of spin fluctuations as $T \to T_N^+$. Below T_N, however, we do not observe the oscillations in the asymmetry spectra usually associated with long-range order. Although this could originate from a broad distribution of the local dipolar fields (arising from either the existence of a large number of muon locations or a large spread of the magnitude of the ordered moment due to a sizable impurity (defect) concentration), the high temperature exponential behaviour largely rules out this explanation. Alternatively, the negligible static dipolar fields at the muon site(s),

[6] An Orbach process is a resonant process that implies a single spin flip ($\hbar\omega_0$), the absorption of a phonon of energy Δ (the energy of the exited CF state) and the emission of a phonon of energy $\Delta + \hbar\omega_0$. It dominates over Raman relaxation when $\Delta \ll k_B\theta_D$, which is typically the case in rare-earth compounds.

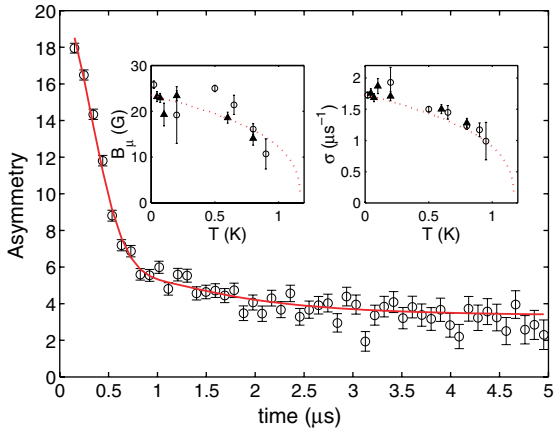

Figure 4. Fit to equation (3) of ETO data at 45 mK. Inset: thermal evolution of the estimated values of the average local field (B_μ) and the transverse relaxation rate (σ). The error bars are just the return from the fitting algorithms. The dotted curves are a guide to the eye.

and hence the absence of oscillations in the depolarization spectra, may possibly be attributed to the high symmetry of the pyrochlore lattice, which can cancel out the fields generated by the Er^{3+} moments.

As in other oxide systems, the muons are expected to localize close to the oxide ions. In the cubic pyrochlore lattice (space group = $F\bar{3}dm$; standard setting), the oxygen anions are located at two crystallographic positions: 8a and 48f, and a calculation of the local dipolar fields at these sites in the ψ_2 spin structure with μ (Er^{3+}) = 3.01 μ_B shows that the field does indeed vanish at the 8a position (and reaches a value of ∼2600 G at 48f). However, muons do not stop precisely at the oxygen positions but are usually considered to reside at a distance of 1 Å away from them [16], in which case the internal field rises up to values of ∼5000–17 000 G along the main crystallographic directions from the 8a position. For the 48f site, on the other hand, the field adopts a minimum value of ∼600 G about 1 Å away along $\langle\bar{1}00\rangle$. A detailed calculation of the muon stopping site(s) and associated values of the local field B_μ is thus required before a definitive answer can be produced. However, we argue that our preliminary calculations and the high temperature behaviour suggest that the high symmetry of the lattice could be responsible for the (partial) cancellation of the internal fields below the transition.

Our present data, however, do not allow us to establish whether this cancellation is complete ($B_\mu = 0$) or just partial, with small but finite B_μ. In the light of the neutron results, which show the onset of long-range antiferromagnetic ordering, ETO ZF data below T_N have been fitted to the function

$$A(t) = A_\perp \exp(-\sigma^2 t^2)\cos(2\pi\nu t) + A_\parallel \exp(-\lambda_\parallel t) + a_{bg}, \tag{3}$$

which characterizes the response of an ordered powder sample. The first term accounts for the signal due to those muons with spin components perpendicular to the quasi-static local magnetic field. Here, the precession frequency $2\pi\nu = \gamma_\mu B_\mu$ (where γ_μ is the muon gyromagnetic ratio $\equiv 2\pi \times 135$ MHz T^{-1}) and the relaxation rate $\sigma = \gamma_\mu \Delta B_\mu$ (where ΔB_μ is the second moment of the local field distribution). The second term reflects the contribution from those muons with spin components parallel to the local field and is characterized by a relaxation rate $\lambda_\parallel$ attributable to dynamic fluctuations of the local field. The ratio $A_\perp$:$A_\parallel \approx$ 2:1, as expected for complete polycrystalline averaging. The fit of the 0.045 K data, shown in figure 4, yields $B_\mu \simeq 23$ G and $\sigma = 1.75(2)$ MHz, corresponding to $\Delta B_\mu \simeq 130$ G. Similar fits at

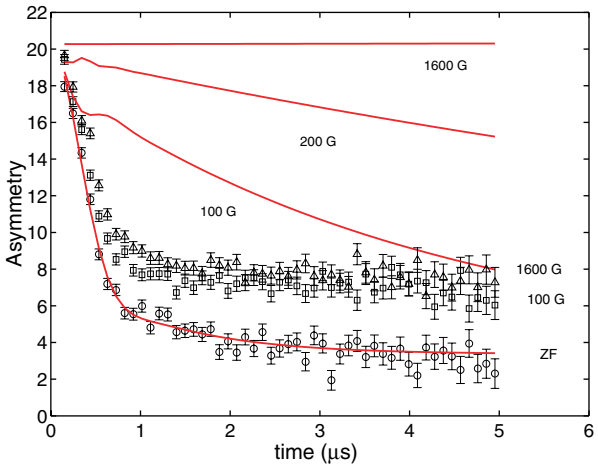

Figure 5. Longitudinal field dependence of the relaxation curves for ETO at 45 mK. Solid curves are predictions by a dynamical Kubo–Toyabe relaxation function, which provides an equally satisfactory description to the ZF data below T_N as equation (3).

different temperatures yield the thermal evolution of the two parameters plotted in the inset of figure 4.

The situation in the ordered phase, thus, appears to be one in which the oscillatory pattern induced by an already small average local field (due to the high symmetry of the system) is washed out by the large distribution width and, to a lesser extent, the persistence of dynamic electronic fluctuations. However, the data can be equally described by a dynamic Kubo–Toyabe function [17] with $\Delta B_\mu \simeq 170$ G (see figure 5), thus introducing the possibility that the local field at the muon site may be entirely cancelled out, despite the fact that our calculations have not shown any plausible site where this occurs. Given the relative sizes of B_μ and ΔB_μ derived from the fits to equation (3), it is not at all surprising that a clear-cut distinction between these two interpretations is not attainable from the data. In any case, the spectra are consistent with the developing of persistent static correlations below 1.1 K, which are responsible for the Gaussian early-time signal ($\beta \sim 2$), in contrast with the exponential shape ($\beta \sim 1$) observed above the transition, characteristic of a rapidly fluctuating system, $\nu \gg \gamma_\mu \Delta B_\mu$.

Finally, an increase in $P_z(\infty)$ (corresponding to up to approximately 10% of the total asymmetry at 45 mK) develops for $T < 0.8$ K, significantly below the ordering temperature. This component is not accounted for by any of the functions above (in fact, due to its size it is difficult to treat it as anything but a rise of the background level) and suggests the presence of at least one other magnetically inequivalent site with a μ^+ population of roughly 10% of that of the majority one.

4.2. Longitudinal-field measurements

Longitudinal field (LF) measurements for ETO are shown in figure 5. LF measurements are commonly used to distinguish between dephasing (due to a static distribution of local fields) and relaxation (due to dynamic fluctuations) of the muon-spin polarization. In the static case, the applied LF increases the proportion of muons whose spin retain the initial orientation along z, causing an increase in the final value of the polarization $P_z(\infty)$. Relaxation caused by fluctuating fields, on the other hand, is not affected by the moderate LF as long as the Zeeman energy of the applied field does not exceed the exchange coupling.

The LF results cannot be easily matched to the findings from the ZF measurements (especially the Gaussian decay of early times). ZF data have shown that the fast initial depolarization is mainly caused by a wide distribution of local fields in the majority muon site, and so, for the derived values of the local field, one would expect the signal to be completely saturated by an LF of around 500 G. The solid curves in figure 5 show the expected evolution of the signal in different LF if it were described by a dynamical Kubo–Toyabe function with the parameters fixed to its ZF values (though the strongly damped oscillation that we have favoured in our analysis above should show a very similar evolution to that of the KT function given the small size of the average field). Instead, partial decoupling occurs for fields up to 100 G, above which depolarization curves overlap for LF up to at least 1600 G. This suggests that two superimposed independent muon relaxation channels are present in ETO below T_N: a small fraction static one that is completely decoupled by LF $\sim$ 100 G and a large fraction dynamical one that is essentially unaffected by an LF of 1600 G. These two components could correspond to two distinct muon sites as suggested by the ZF measurements, with the undecouplable one being related to the majority site, in contrast to expectations from the ZF analysis.

ETO thus appears to provide a new example of the 'undecouplable Gaussian' relaxation that has been previously observed in other frustrated systems such as the Kagomé material $SrCr_xGa_{12-x}O_{19}$ (SCGO). In SCGO a similar Gaussian relaxation was observed which also did not couple in available longitudinal fields; such an effect is surprising since a Gaussian relaxation is usually associated with a static field distribution which is then easily decoupled. Undecouplable relaxation is associated with dynamics but dynamical processes usually give rise to exponential, not Gaussian, relaxation. The mechanism posited to explain the relaxation in SCGO was the presence of a non-persistent fluctuating field, which is often zero but sporadically becomes non-zero [18]. This can be shown to produce the required undecouplable Gaussian relaxation and, in SCGO, it can be linked to a spin liquid ground state in which the 'zeroing' of the local field is due to the formation of *local* spin singlet pairs. A similar or related effect may thus be important for ETO.

4.3. Behaviour of $\lambda_\parallel(T)$ as $T \to 0$ from ZF measurements

A remarkable feature of our ETO results is the persistence of a non-vanishing dynamical relaxation rate $\lambda_\parallel$ at low temperature, contrary to what is expected for a conventional long-range ordered magnet where magnetic excitations die out as $T \to 0$. Instead, $\lambda_\parallel$ remains finite and temperature independent, suggesting a finite density of low-lying excited states down to the lowest temperature. A temperature-independent relaxation rate has been reported before for other geometrically frustrated magnets, most of which, however, unlike ETO, show a disordered or glassy state at low temperatures [18–20]. Recently, low temperature saturation of $\lambda(T)$ has been reported by Yaouanc and co-workers on the Heisenberg system $Gd_2(Ti, Sn)_2O_7$, with long-range AFM order below $T_N \sim 1$ K. Considering relaxation via a Raman scattering process involving two magnons (direct single-magnon events are prevented at this temperature by energy conservation considerations), the authors conclude that the T-independence of the relaxation rate is only attainable if there is a density of states with a temperature-dependent gap [21]. Inelastic neutron scattering results for ETO do indeed suggest a gapped magnon spectrum in this material with a gap of $\Delta/k_B \sim 4$ K at 100 mK (although there is no direct evidence of a temperature dependence of Δ). However, this finding is in contradiction with the T^3-dependence of the specific heat at low temperatures, which indicates a quadratic density of states with no associated gap. The T^3-dependence could therefore arise from a 'hidden' branch of excitations that do not couple to the neutrons but do show up in the specific heat. A similar situation arises in the quasi-two dimensional system SCGO, with $\sim T^2$ specific heat despite

the absence of conventional magnons. In fact, μ^+SR [22] and heat capacity [23] results for SCGO indicate that the fluctuations that persist below T_{sg} are of local nature. Hence, although further work is needed to understand the nature of the dynamics below T_N in $Er_2Ti_2O_7$, the present evidence suggests that a Raman process involving spin waves might not be the relevant mechanism to explain the μ^+SR response at low temperature in the present system. The behaviour of $Er_2Sn_2O_7$ (see the following section), which has a similar evolution of λ, also points in that direction.

5. Low temperature behaviour: $Er_2Sn_2O_7$

For ESO, the depolarization spectra remain exponential ($\beta \simeq 1$) down to 0.02 K (see figure 2(b)), suggesting the dynamic nature of the local field modulation, in agreement with previous susceptibility results that indicate that this material does not order magnetically at finite temperature [10]. Despite this, the low temperature evolution of $\lambda(T)$ closely resembles that of the Ti material, with a relatively sharp slowing down of spin fluctuations occurring at roughly the same temperature for both materials (figure 3), which suggests strong similarities in the behaviour of the spin fluctuations. The exponential relaxation in ESO may not necessarily preclude magnetic order, particularly if the muon stops at a site of high symmetry in which the field from neighbouring Er3+ moments cancels and the relaxation results from randomly distributed dilute faults. Nevertheless, the absence of a shape change from $\beta \approx 1$ to $\beta \approx 2$, as found in ETO, makes a magnetic transition less likely. Further neutron, μ^+SR and calorimetric measurements on mixed Ti/Sn materials are planned and may shed some light on some of these issues.

6. Conclusions

We have presented a μ^+SR study of spin dynamics in the systems $Er_2Ti_2O_7$ (ETO) and $Er_2Sn_2O_7$ (ESO) that corroborate previous results regarding ordering in these materials and shed some new light into their low temperature state. Thus, we find that for ETO a persistent static component develops below $\sim$1.1 K, whereas ESO remains dynamic down to 0.02 K. For ESO, the spin system undergoes a relatively sharp slowing down at the same temperature as for ETO. The absence of the oscillations in the ordered phase of ETO is attributed to the high symmetry of the magnetic sublattice, which greatly reduces the magnitude of the average local field so that, as a result, even a relatively narrow distribution of local fields and remaining spin dynamics are able to wash out the oscillations entirely. In contrast to expectations for a conventional magnet, ETO shows non-vanishing spin dynamics as $T \to 0$. The nature of these dynamics is not yet known, but the rather similar thermal dependence of λ for both ETO and ESO, along with previous specific heat and neutron results, suggests that the excitations involved are not collective spin waves about the ordered state but might instead be of local nature, largely independent of the onset of long-range order.

Acknowledgments

This work was performed at the Swiss Muon Source, Paul Scherrer Institute, Villigen, Switzerland and the ISIS Pulsed Muon Facility, RAL, UK. The authors would like to thank the staff of PSI and ISIS for technical assistance. JL wants to thank the Basque Government for a post-doctoral research grant. We acknowledge funding from the EPSRC (UK).

References

[1] Gardner J S, Gaulin B D, Greedan J E, Lumsden M D, MacFarlane W A, Raju N P, Sonier J E, Swainson I and Tun Z 1999 *Phys. Rev. Lett.* **82** 1012
[2] Harris M J, Bramwell S T, McMorrow D F, Zeiske T and Godfrey K W 1997 *Phys. Rev. Lett.* **79** 2554
[3] Bramwell S T and Gingras M J P 2001 *Science* **294** 1495
[4] Bramwell S T, Gingras M J P and Reimers J N 1994 *J. Appl. Phys.* **75** 5523
[5] Champion J D M *et al* 2003 *Phys. Rev.* B **68** 020401
[6] Champion J D M and Holdsworth P C W 2003 *J. Phys.: Condens. Matter* **16** S665
[7] Villain J 1980 *J. Physique* **41** 1263
[8] Rams M and Hodges J A 2003 private communication
[9] Blöte H W J, Wielinga R F and Huiskamp W J 1969 *Physica* **43** 549
[10] Matsuhira K, Hinatsu Y, Tenya K, Amitsuka H and Sakakibara T 2002 *J. Phys. Soc. Japan* **71** 1576
[11] Blundell S J 1999 *Contemp. Phys.* **40** 175
[12] Dalmas de Réotier P, Yaouanc A, Gubbens P C M, Kaiser C T, Baines C and King P J C 2003 *Phys. Rev. Lett.* **91** 167201
[13] Finn C P B, Orbach R and Wolf W P 1961 *Proc. Phys. Soc.* **77** 261
[14] Orbach R 1961 *Proc. Phys. Soc.* **77** 821
[15] Carlin R C and van Duyneveldt A J 1977 *Magnetic Properties of Transition Metal Compounds* (Berlin: Springer)
[16] Li Q and Brewer J H 1990 *Hyperfine Interact.* **63** 169
[17] Hayano R S, Uemura Y J, Imazato J, Nishida N, Yamazaki T and Kubo R 1979 *Phys. Rev.* B **20** 850
[18] Uemura Y J *et al* 1994 *Phys. Rev. Lett.* **73** 3306
[19] Marshall I M, Blundell S J, Pratt F L, Husmann A, Steer C A, Coldea A I, Hayes W and Ward R C C 2002 *J. Phys.: Condens. Matter* **14** L157
[20] Dunsiger S R *et al* 1996 *Phys. Rev.* B **54** 9019
[21] Yaouanc A, Dalmas de Réotier P, Bonville P, Hodges J A, Gubbens P C M, Kaisel C T and Sakarya S 2003 *Physica* B **326** 456
[22] Keren A, Uemura Y J, Luke G, Mendels P, Mekata M and Asano T 2000 *Phys. Rev. Lett.* **84** 3450
[23] Ramirez A P, Hessen B and Winklemann M 2000 *Phys. Rev. Lett.* **84** 2957